


FULL ARTICLE

Non-invasive optical method for real-time assessment of intracorneal riboflavin concentration and efficacy of corneal cross-linking

Giuseppe Lombardo^{1,2*}  | Valentina Villari¹ | Norberto L. Micali^{1*} | Nancy Leone¹ | Cristina Labate³ | Maria P. De Santo³ | Marco Lombardo²

¹Dipartimento Scienze Chimiche e Tecnologie dei materiali, CNR-IPCF, Istituto per i Processi Chimico Fisici, Messina, Italy

²Vision Engineering Italy srl, Rome, Italy

³Dipartimento di Fisica, Ponte P. Bucci, Università della Calabria, Calabria, Italy

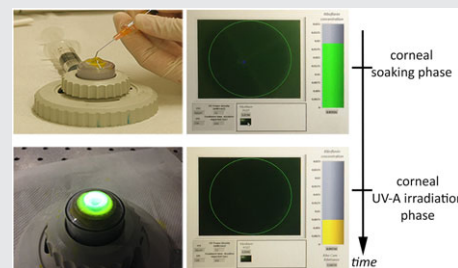
*Correspondence

Giuseppe Lombardo, CNR-IPCF, Istituto per i Processi Chimico-Fisici, Viale F. Stagno D'Alcontres 37, 98158 Messina, Italy.
Email: giuseppe.lombardo@cnr.it

Norberto L. Micali, CNR-IPCF, Istituto per i Processi Chimico-Fisici, Viale F. Stagno D'Alcontres 37, 98158 Messina, Italy.
Email: micali@me.cnr.it

Keratoconus is the primary cause of corneal transplantation in young adults worldwide. Riboflavin/UV-A corneal cross-linking may effectively halt the progression of keratoconus if an adequate amount of riboflavin enriches the corneal stroma and is photo-oxidated by UV-A light for generating additional cross-linking bonds between stromal proteins and strengthening the biomechanics of the weakened cornea.

Here we reported an UV-A theranostic prototype device for performing corneal cross-linking with the ability to assess corneal intrastromal concentration of riboflavin and to estimate treatment efficacy in real time. Seventeen human donor corneas were treated according to the conventional riboflavin/UV-A corneal cross-linking protocol. Ten of these tissues were probed with atomic force microscopy in order to correlate the intrastromal riboflavin concentration recorded during treatment with the increase in elastic modulus of the anterior corneal stroma. The intrastromal riboflavin concentration and its consumption during UV-A irradiation of the cornea were highly significantly correlated ($R = 0.79$; $P = .03$) with the treatment-induced stromal stiffening effect. The present study showed an ophthalmic device that provided an innovative, non-invasive, real-time monitoring solution for estimating corneal cross-linking treatment efficacy on a personalized basis.



KEYWORDS

corneal cross-linking, fluorescence, riboflavin, theranostics, UV-A device

1 | INTRODUCTION

Keratoconus is a progressive, bilateral, ectatic corneal disease, characterized by stromal thinning and weakening that leads to corneal distortion. Estimates of the rates for keratoconus range from 1 in 500 to 1 in 2500 people depending upon the geographic location. The aetiology of this disease

is multifactorial; it represents the final common pathway for a variety of different pathological processes [1–4]. Visual loss occurs in the second-third decades of life, primarily from irregular astigmatism and myopia, and secondarily from corneal scarring. Currently, keratoconus represents the primary cause of corneal transplantation in young adults worldwide.

Over the past decade, riboflavin/UV-A corneal cross-linking has become an established treatment option for slowing down or halting the progression of keratoconus [5–8]. The procedure aims to strengthen the biomechanical stability of the weakened cornea. The efficacy of corneal cross-linking via UV-A irradiation of the cornea saturated with riboflavin has been primarily demonstrated by laboratory studies showing that the procedure increases the biomechanical strength of the treated cornea [9–12]. The adequate bioavailability of riboflavin in the corneal stroma prior to UV-A illumination and its effective consumption during corneal UV-A illumination represent the two primary factors for achieving effective outcomes in patients [13, 14].

In clinic, efficacy of corneal cross-linking is assessed by comparing post-operative corneal topography with baseline measurements over at least 1-year follow-up [8, 15, 16]. However, patients usually wear contact lenses, which alter the shape of the cornea and often make the estimation of keratoconus progression during post-operative follow-up challenging. Real-time monitoring of treatment efficacy (e.g., monitoring intracorneal riboflavin concentration) would be desirable, as it would be possible to tailor a precise treatment to every patient's eye. Such approach would be desirable especially in paediatric patients, who represent a population at high risk for more rapid progression of keratoconus. At present, uncertainty in treatment outcomes derives from many variables that are both related to the individual patient's corneal tissue, such as the differences in penetration of riboflavin into the corneal stroma and consumption of intrastromal riboflavin during UV-A irradiation, and to the number of different treatment protocols at the surgeon's disposal [17, 18].

The intrastromal riboflavin concentration has been measured with accuracy in the laboratory using spectrophotometry, high performance liquid chromatography, confocal fluorescence microscopy and two-photon optical microscopy [13, 14, 19, 20]. Nevertheless, these techniques are invasive and cannot be directly translated to the clinic. Friedman et al. [21] have realized an UV-A device utilizing a digital micromirror device (DMD) and a fluorescent dosimetry camera. The DMD has been configured for switching between the UV-A illumination profile intended for cross-linking treatment (10 mm area) and that of a vertical one-pixel line width (25 μm ; 256 levels of intensity) intended for fluorescent dosimetry at intervals prior to and during the treatment; the camera served to collect line images of the cross-sectional distribution of fluorescence due to excited riboflavin through the cornea in porcine eyes. The authors have collected measures of the drop in fluorescence intensity profile of either a whole corneal cross-section image or the most anterior 12 μm of the cornea. They were able to measure a diffusion coefficient for the emitted fluorescence by riboflavin of $3.3 \pm 0.2 \times 10^{-7} \text{ cm}^2/\text{s}$, which was on average 15% lower

than measured using a Franz cell ($3.8 \pm 0.2 \times 10^{-7} \text{ cm}^2/\text{s}$) in the same study [21] and 21% lower if compared with another study by the same group ($4.0 \pm 0.2 \times 10^{-7} \text{ cm}^2/\text{s}$) [22]. However, the authors were unable to provide measures of the intrastromal riboflavin concentration during treatment or any estimation of treatment efficacy.

In this work, we present a theranostic UV-A prototype device that monitors non-invasively the intrastromal concentration of riboflavin during treatment as well as provides estimation of corneal cross-linking efficacy in real time. Theranostics is a new strategy of precision medicine for delivering personalized therapy by examining the effect in real time through in vivo diagnostic imaging. The present device was tested in the laboratory using seventeen eye bank donor human corneal tissues.

2 | MATERIAL AND METHODS

2.1 | Human sclerocorneal tissues

Seventeen total human donor sclerocorneal tissues from different donors were obtained from the Veneto Eye Bank Foundation (Venezia Zelarino, Italy). Inclusion criteria included an endothelial cell density (ECD) ≥ 1800 cells/ mm^2 ; exclusion criteria included any corneal or ocular surgery. The study adhered to the tenets of Declaration of Helsinki for the use of human tissues and was approved by the National Research Council research ethics and bioethics advisory committee.

Seven human donor sclerocorneal tissues were used to assess the novel UV-A device and the optical method in the laboratory; the other 10 donor sclerocorneal tissues were used to correlate data collected by the novel UV-A device during corneal cross-linking with the increased biomechanical strengthening of the anterior stroma induced by treatment.

2.2 | UV-A device optical set-up

The optical set-up of the prototype device is schematized in Figure 1. The UV-A light ($365 \pm 10 \text{ nm}$), generated by a LED (LD), is collimated by lens L_1 and reaches the cornea through the reflection from a long pass dichroic mirror (DM, long pass filter with cut-off wavelength of 410 nm). The residual light passing through DM is measured by a photodiode (PD), which monitors the UV-A power density. The lens L_2 conjugates the corneal plane with the CMOS sensor of the RGB camera (DCC1645C, Thorlabs Inc, Newton, NJ). The camera acquires images of 1280×1024 (pixel size = 3.6 μm). When the cornea is enriched with riboflavin and is excited by UV-A light, the riboflavin fluorescence presents a band of emission spectrum that overlaps the RGB camera's green filter. The intensity values of the green pixels (values range from 0 to 255 levels, ie, 8 bits)

of the corneal image are averaged and this value, I_G , provides a measure of the whole fluorescence contribution, $I_F(\lambda_F)$, at wavelength λ_F , emitted from the cornea soaked with riboflavin. Since I_G and $I_F(\lambda_F)$ are linearly correlated, the exposure and frame rate of the RGB camera are modified in accordance with the UV-A power density in order to ensure the widest dynamic range as possible for each cornea.

A PC, running a custom LabVIEW (National Instruments Corporation, 11500 Mopac Expressway, Austin, TX) routine interfacing with an Arduino μ controller (Arduino LLC; www.arduino.cc), manages the overall operation of the theranostic UV-A device; it turns on/off LD and changes its power density, monitors the intensity of PD, acquires the images from the RGB camera and controls its main parameters (ie, frame rate, exposure time, etc.). It then elaborates the acquired information for calculating in real time the intrastromal riboflavin concentration and treatment efficacy. The UV-A device sensitivity, which is assessed by considering the smallest detectable concentration value of riboflavin (corresponding to twice the camera's noise) is $5 \times 10^{-6} \text{ g/cm}^3$. The present device also includes 2 low power alignment red lasers used to move the focal plane onto the cornea.

2.3 | Theoretical outline of fluorescence

The fluorescence intensity, $I_F(\lambda_F)$, is proportional to the spectral emission, $F(\lambda_F)$, whose integral represents the fluorescence quantum efficiency, and to the absorbed light intensity, I_A , at the excitation wavelength, λ_E :

$$I_F(\lambda_F) = h(C, T)F(\lambda_F)I_A(\lambda_E), \quad (1)$$

where $h(C, T)$ is a quenching function, which depends on the riboflavin concentration, C , and on the temperature, T [23]. By introducing in Eq. (1) the riboflavin absorption $a(\lambda_E)$ and the excitation intensity, $I_0(\lambda_E)$, it becomes as follows:

$$I_F(\lambda_F) = h(C, T)F(\lambda_F)I_0(\lambda_E)a(\lambda_E). \quad (2)$$

The fluorescence intensity is proportional to the riboflavin concentration by means of its absorption coefficient, $a(\lambda_E)$. After calibration of the device, which is mandatory to derive $h(C, T)$, and by taking into account the corneal thickness, the fluorescence signal, I_G , can be correlated with the riboflavin concentration. The quenching function, $h(C, T)$, depends non-linearly on T and C , however, for sufficiently low concentrations of riboflavin (typically for $C < 2 \times 10^{-4} \text{ g/cm}^3$), $h(C, T)$ depends linearly on C (T is constant during the UV-A device operation) [24, 25].

2.4 | Theranostic UV-A device calibration

Calibration of the theranostic UV-A device is needed in order to uniquely correlate I_G with the unknown riboflavin

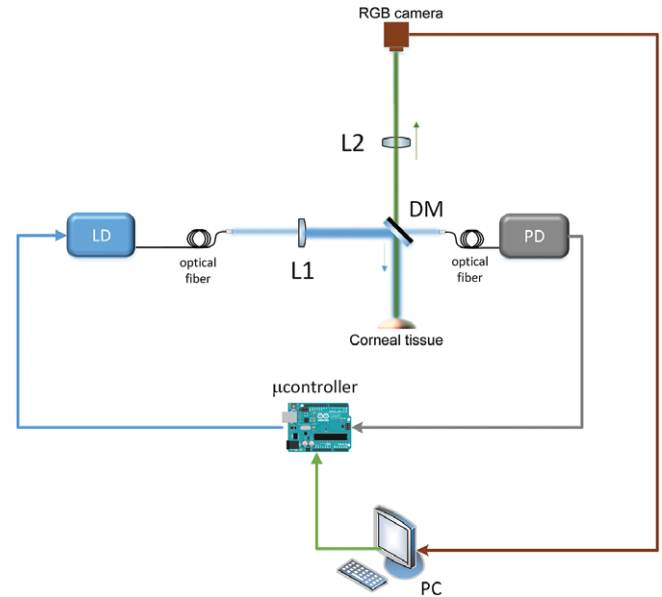


FIGURE 1 Schematic of the UV-A theranostic prototype device. The UV-A LED (LD) illuminates the corneal tissue under treatment; the photodetector (PD) monitors the power density of the UV-A excitation light. The lenses L_1 and L_2 represent the collimation lens and the achromatic doublet lens, respectively; L_2 conjugates the corneal focal plane to the pupil plane of the RGB camera (1280 \times 1024 pixels resolution; 1/3 in. CMOS digital image sensor). The μ controller is an *Arduino Uno* board, which controls the LD power density and acquires voltage signal from PD. The computer (PC), which runs a routine in LabView, manages the overall process of the UV-A device

concentration. The calibration procedure was carried out by using a spectrophotometer (Avaspec 2048L, Avantes BV, Apeldoorn, The Netherlands) [17, 20, 25]. Data were expressed as spectrum of absorbance (or optical density). The extinction coefficient of riboflavin at 445 nm ($\epsilon_{445} = 10\,800/\text{cm M}$) was determined by measuring the absorbance of several riboflavin dilutions, ranging from 5×10^{-6} to $3.5 \times 10^{-4} \text{ g/cm}^3$. Then, the calibration curve was obtained by associating at each concentration value, measured by the absorption spectrum, the value acquired and processed by the device, I_G , which defines the fluorescence emitted by the riboflavin in the corneal stroma, $I_F(\lambda_F)$. In this study, the concentration of riboflavin was expressed as g/cm^3 or as percentage (%), where $1 \times 10^{-4} \text{ g/cm}^3$ corresponds to 0.010%.

2.5 | Corneal cross-linking treatment and UV-A device operation

Seven sclerocorneal tissues were treated by using the novel theranostic UV-A device. Donors (64 ± 6 years) did not have history of corneal pathologies or eye surgery. The tissues were explanted between 3 and 20 hours post-mortem and cultivated at 30°C in corneal storage medium for 2 weeks. The mean cadaver time was 10 ± 6 hours. The ECD ($2257 \pm 336 \text{ cells/mm}^2$) was measured using an inverted optical microscopy (Axiovert 25, Carl Zeiss

Microscopy, Jena, Germany). The sclerocorneal samples were shipped to the laboratory in 6% dextran-enriched corneal storage medium and were used for experiment within 24 hours.

Each sclerocorneal tissue was placed in an artificial anterior chamber (AAC, Coronet, Network Medical Products, Ltd, North Yorkshire, UK), pressurized with the AAC filled with 0.9% sodium chloride using a 5 mm syringe and treated according to clinical guidelines. Before removing the corneal epithelium with an Amoils' brush (Innovative Excimer Solutions Inc., Toronto, ON), the central corneal thickness (CCT; $544 \pm 103 \mu\text{m}$) was measured with an ultrasound corneal pachymeter (Pachmate, DGH, Exton, PA); thereafter, each corneal tissue was treated according to the Dresden protocol [6–8]. Briefly, this gold standard protocol consists of soaking the cornea with riboflavin for 30 minutes before irradiating the tissue at 3 mW/cm^2 for 30 minutes with an irradiation area of 9 mm diameter. In this work, we used a 20% dextran enriched 0.1% riboflavin (Ricrolin, Sooft Italia SpA, Montegiorgio (FM), Italy) instilled every 2 to 3 minutes before UV-A irradiation. The only exception with the Dresden protocol was that no riboflavin drops was added during irradiation in order to avoid any bias in the estimation of riboflavin by the theranostic device.

Before commencing each treatment, the native corneal fluorescence (ie, the background or baseline corneal reference signal, B_G), was acquired from each tissue. This value was then subtracted from the fluorescence emitted by the cornea during treatment (either during soaking or UV-A irradiation of the cornea). After 30 minutes of stromal soaking with riboflavin, the excess of riboflavin was gently washed from the stromal surface of the cornea using a sodium chloride 0.9% solution in order to measure only the intrastromal riboflavin. The intrastromal riboflavin concentration was derived from the calibration curve by measuring I_G when the cornea was illuminated with an UV-A irradiation at very low power density ($<0.6 \text{ mW/cm}^2$) in order not to induce any photodynamic polymerization process of the corneal stroma. Each corneal tissue was then irradiated at 3 mW/cm^2 for 30 minutes. During UV-A illumination of the cornea, the intrastromal riboflavin concentration was again evaluated from the calibration curve by measuring the acquired I_G value. This procedure permitted to measure the intrastromal riboflavin consumption during the irradiation of the tissue. No additional riboflavin was applied during irradiation (Figure 2).

The riboflavin concentration values computed by the theranostic UV-A device were compared with that measured independently from the absorbance with the spectrophotometer both at the end of corneal soaking and at the end of UV-A illumination of the cornea [13, 14]. Any potential loss in light transmission due to the quartz microscope slide and to the refractive index mismatch between the corneal

tissue and air was minimized because each cornea was measured under the same conditions before and after corneal soaking with riboflavin and after UV-A irradiation. The intraclass correlation coefficient (ICC; two-way random effects model) was calculated in order to estimate the absolute agreement between intrastromal concentrations of riboflavin calculated with the 2 independent optical methods.

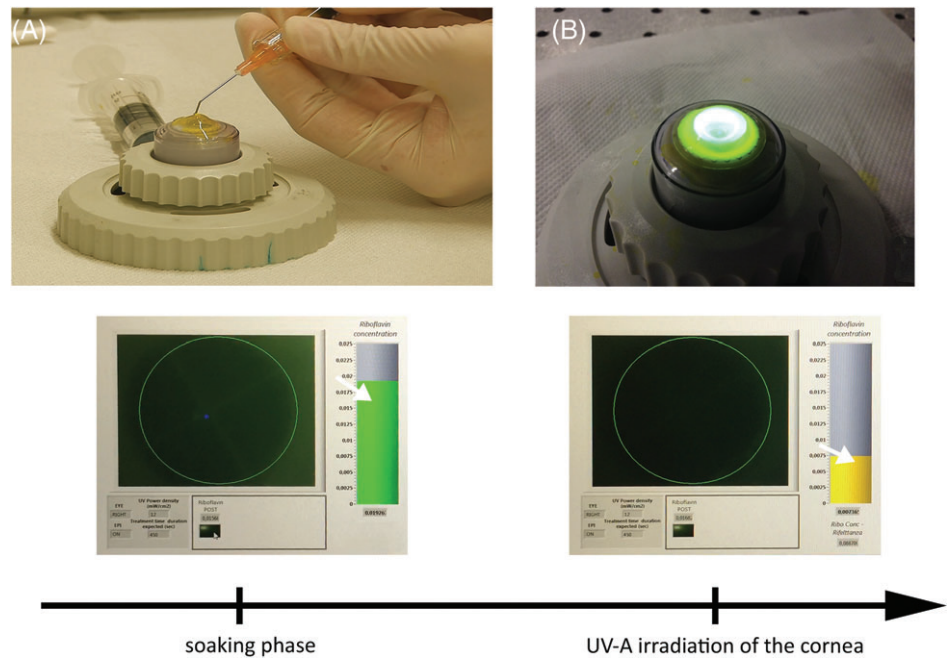
2.6 | Biomechanical testing

The mechanical properties of the anterior stroma of 10 eye bank donor sclerocorneal tissues from different donors obtained from the Veneto Eye Bank Foundation (donor age: 63 ± 8 years; cadaver time: 10 ± 4 hours; ECD: $2000 \pm 190 \text{ cells/mm}^2$; CCT: $528 \pm 29 \mu\text{m}$) were probed by atomic force microscopy (AFM) before and after corneal cross-linking with the novel UV-A device. The Amoils' brush was used to remove the corneal epithelium; each corneal tissue was then soaked with 20% dextran enriched 0.1% riboflavin (Ricrolin, Sooft Italia SpA) for 30 minutes before UV-A irradiation at 3 mW/cm^2 for 30 minutes. One drop of riboflavin was applied every 3 to 5 minutes over the cornea during irradiation in order to mimic the approach of eye surgeons, who apply drops for protecting the tissue by possible UV-A phototoxic effects on the corneal endothelium [5–8]. An expert corneal surgeon (M.L.) performed all the treatments in order to replicate the standard clinical operating procedure in the laboratory.

During AFM measurements, each corneal tissue was gently placed on a specially designed Teflon environmental cell with the endothelial side facing downward and kept in place without the use of glue to preserve its mechanical properties. A NanoScope IIIa atomic force microscope (Bruker, Billerica-MA, USA) was operated in the Force Spectroscopy mode to analyze the Young's modulus of elasticity of the most anterior stroma. Measurements were performed at 27°C (close to the physiological temperature of the human cornea), with the specimens immersed in 20% dextran solution, using phosphorus-doped rectangular silicon cantilevers of nominal elastic constant between 20 and 80 N/m (TESPA, Bruker). Dextran was used as imaging medium to keep the tissues at the same osmolarity of riboflavin/UV-A corneal cross-linking [11]. The nominal value of the tip radius of curvature was 10 nm. Force curves were obtained on 3 different locations at the centre of the anterior stroma of each sample and several force curves (30 curves for each rate) were recorded at the approach speed of $3.5 \mu\text{m/s}$ at each location. No adhesion between the tip and the sample surface was detected in any sample. We made sure to avoid any possible alteration of the tissue during measurement; any rupture in the material would have induced a discontinuity in the force curve profile and therefore would have been clearly identified [26].

Calibration of both the AFM optical sensitivity and the spring constant of each cantilever was done, as previously

FIGURE 2 Main steps of the experiments performed in the present study. Standard corneal cross-linking with riboflavin was performed using the theranostic UV-A prototype device. (A) Each cornea was mounted in the AAC and soaked with 20% dextran-enriched 0.1% riboflavin solution for 30 minutes. (B) The cornea was then irradiated at 3 mW/cm^2 for 30 minutes. The theranostic UV-A device provided a real-time estimation of intrastromal riboflavin concentration during treatment. The arrows point out the tank showing the intrastromal concentration of riboflavin during soaking phase and UV-A irradiation phase. The different colour correlated with the amount of intrastromal riboflavin concentration, that is, green for concentration above 0.016% ($1.6 \times 10^{-4} \text{ g/cm}^3$), yellow for concentration below 0.008% ($0.8 \times 10^{-4} \text{ g/cm}^3$)



described in detail [11, 26, 27]. We determined the physical constants (ie, length, width and thickness) of each cantilever and the optical detector sensitivity. From these experimental calibrations, the spring constant of the cantilevers used in the experiment was 45 N/m .

The Young's modulus of elasticity (E) was calculated individually for each corneal sample before and after cross-linking. The Young's modulus was calculated by fitting the approach curve with the Hertz-Sneddon model for a conical indenter [11, 26–29]. This model relates the loading force to indentation, which for a conical indenter is:

$$F = F_0 + \frac{2}{\pi} \frac{E}{1-\nu^2} (\delta - \delta_0)^2 \tan(\alpha), \quad (3)$$

where F is the loading force in Newton (N), ν is the Poisson's ratio (0.49 for the corneal tissue), δ is the indentation depth, E is the Young's modulus in Pascal, F_0 and δ_0 are the loading force at baseline and the indentation depth at the contact point, respectively. A custom software written in Matlab permitted to identify automatically the contact point and thus to provide a reproducible value of E , as previously shown [11, 26, 30].

The Student's t -test was used to compare the Young's modulus values collected before and after riboflavin/UV-A corneal cross-linking. In addition, the biomechanical results were correlated with the riboflavin concentration values measured by theranostic prototype device during treatment. A regression curve was developed to correlate the increment of stromal stiffness as a function of riboflavin concentration:

$$Y = b_0 + b_1 C_{\text{post}} + b_2 C_{\text{consumption}\%}, \quad (4)$$

where C_{post} is the intrastromal concentration of riboflavin after stromal soaking and $C_{\text{consumption}\%}$ is the ratio of the

differences between C_{post} and the intrastromal riboflavin concentration after UV-A irradiation of the cornea, $C_{UV-A3mW}$ and C_{post} , and b_0 , b_1 and b_2 are the coefficients of regression.

3 | RESULTS

After 30 minutes of stromal soaking, the intrastromal riboflavin concentration was highly consistent between tissues ($0.014 \pm 0.003\%$). After UV-A irradiation of the cornea, the mean intrastromal riboflavin concentration was $0.003 \pm 0.001\%$; the mean consumption of riboflavin was $80 \pm 4\%$. During UV-A irradiation, the stromal riboflavin concentration decreased non-linearly in all tissues (Figure 3).

The intrastromal riboflavin concentration, determined by fluorescence and absorbance spectrum measurements, after stromal soaking and UV-A irradiation of the cornea is summarized in Table 1. After stromal soaking, the results obtained with the two optical methods showed good agreement ($\text{ICC} = 0.60$; $P = .05$). The absolute agreement between the two methods decreased after UV-A irradiation of the cornea ($\text{ICC} = 0.32$; $P = .01$), caused by tissue shrinking (corneal stroma thinned averagely by 29% after treatment) and increased back-scattered light from the tissue, which made the absorption measurements less reliable than fluorescence measurements.

After conventional riboflavin/UV-A corneal cross-linking, the Young's modulus increased significantly from $1.61 \pm 0.53 \text{ MPa}$ preoperatively to $2.08 \pm 0.72 \text{ MPa}$ postoperatively ($P = .001$). The biomechanical strengthening of the anterior stroma was significantly correlated with the amount of intrastromal riboflavin measured immediately before UV-A irradiation and with the consumption of

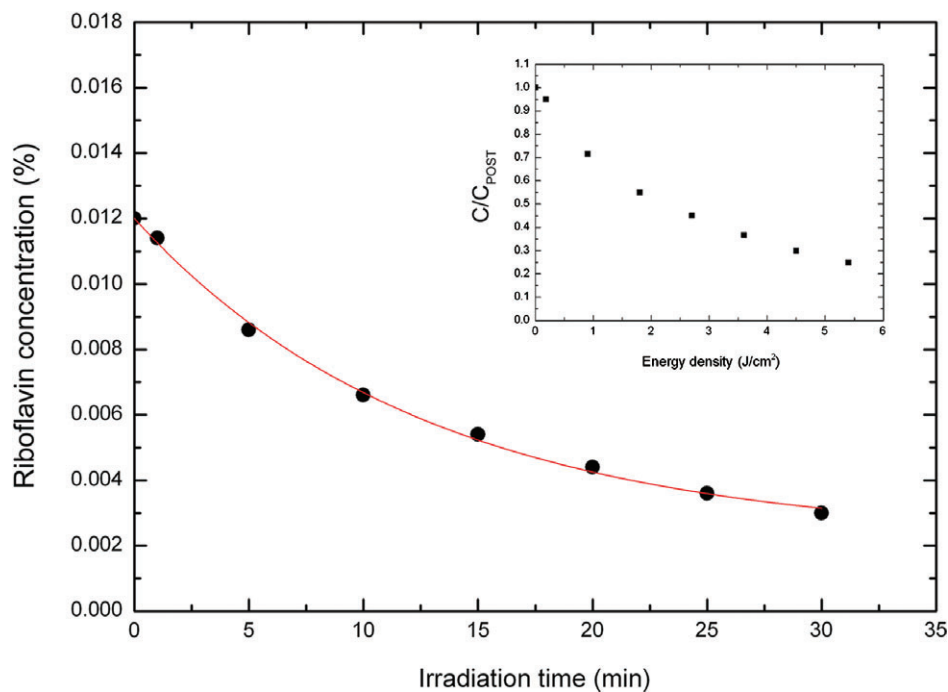


FIGURE 3 Consumption of intrastromal riboflavin during UV-A illumination at 3 mW/cm^2 for 30 minutes in a representative case (tissue 153 420). The lines are the results of the fit with an exponential law, $C(t) = C_{\text{post}} \exp(-t/\tau)$, which yields the rate, τ , of intrastromal riboflavin consumption (12.8 minutes). The inset shows the intrastromal riboflavin concentration during UV-A irradiation normalized to C_{post} as a function of the UV-A energy density

intrastromal riboflavin by UV-A irradiation of the cornea. The result of the model was highly statistically significant ($R = 0.79$; $P = .03$; Figure 4). In all cases that had a regression value of 1.3 (ie, E increased by 1.3 times) C_{post} and $C_{\text{consumption}\%}$ were $>0.014\%$ and $>65\%$, respectively. The various riboflavin drops administration over the corneal stroma during UV-A irradiation (1 drop every 3-5 minutes), as currently done in the standard clinical operating procedure, was valuable to generate differences among tissues; the consumption of riboflavin during UV-A irradiation differed significantly among samples and was the primary cause of the differently induced treatment stiffening effect (Table 2).

4 | DISCUSSION

We disclosed a novel apparatus for performing corneal cross-linking that measures non-invasively the intrastromal

TABLE 1 Corneal intrastromal riboflavin concentration immediately after stromal soaking (C_{post}) and after UV-A irradiation of the cornea using 3 mW/cm^2 for 30 minutes ($C_{\text{UV-A}3\text{mW}}$) determined by the theranostic UV-A device (fluorescence) and by spectrophotometry (absorbance)

Corneal tissue	Fluorescence		Absorbance	
	C_{post} (10^{-4} g/cm^3)	$C_{\text{UV-A}3\text{mW}}$ (10^{-4} g/cm^3)	C_{post} (10^{-4} g/cm^3)	$C_{\text{UV-A}3\text{mW}}$ (10^{-4} g/cm^3)
153 420	1.2	0.3	1.8	0.8
153 769	1.2	0.3	1.5	0.7
151 978	1.6	0.3	1.3	0.5
151 979	1.4	0.3	1.5	0.7
153 865	1.1	0.2	1.3	0.7
160 227	1.8	0.4	2.7	0.9
160 289	1.4	0.3	1.7	0.6
M \pm SD	1.4 ± 0.3	0.3 ± 0.1	1.7 ± 0.4	0.7 ± 0.2

riboflavin concentration of the cornea and provide biomarkers of treatment efficacy in real time.

The performance of the device was evaluated by testing human donor corneal tissues and comparing the results with those obtained by absorption measurements, which represents the state-of-the-art optical technology for measuring the UV absorption of riboflavin [13, 14, 31–34]. Absorption spectrum allows for the determination of the intrastromal riboflavin concentration from the known value of the molar extinction coefficient of riboflavin [13, 14]; due to its invasiveness, however, it cannot be used directly in patients. Furthermore, absorption spectrum is affected by tissue's structure and optical properties, which may lead to unreliable measurements, as found in this study after UV-A irradiation of the cornea. The disclosed UV-A device does not suffer from these limitations because it is based on fluorescence measurements of excited intracorneal riboflavin. The image data acquired by the novel UV-A device were reliable to determine non-invasively the intrastromal concentration of riboflavin during corneal cross-linking and were consistent with previous studies, which used different optical techniques [13, 14, 32].

In order to test the hypothesis that C_{post} and $C_{\text{consumption}\%}$ were key factors to achieve effective outcome of corneal cross-linking, we correlated these measurements with the induced stiffening effect on the anterior stroma of 10 eye bank donor tissues. After treatment, the Young's modulus of elasticity of the anterior stroma increased by 1.02 to 1.58 times in comparison with baseline measurements, which showed a fair agreement with previous studies [9–12, 35]. The increased biomechanical strengthening of the stroma was highly significantly correlated with the intrastromal concentration of riboflavin prior to UV-A illumination of

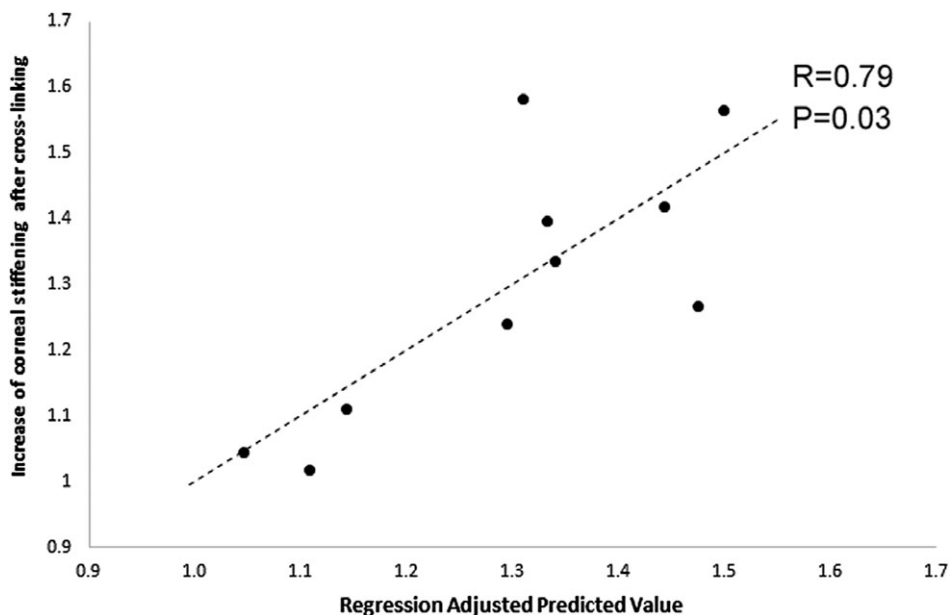


FIGURE 4 Correlation between the mechanical stromal stiffening induced by conventional corneal cross-linking and that predicted by a two-predictor model incorporating the intrastromal concentration of riboflavin (C_{post}) after 30 minutes of soaking and the consumption of intrastromal riboflavin during UV-A irradiation ($C_{\text{consumption}\%}$). Each symbol represents a human donor corneal tissue ($n = 10$)

the cornea and the consumption of intrastromal riboflavin caused by UV-A illumination of the cornea. The small increase of the Young's modulus of elasticity of the anterior stroma in 30% of tissues was correlated with the lower consumption of intrastromal riboflavin during UV-A irradiation ($C_{\text{consumption}\%} \leq 50\%$), likely caused by the masking effect of 20% dextran enriched 0.1% riboflavin drops applied over the stromal surface during irradiation, as shown previously [13]. Differences between samples could be primarily caused by (1) more frequent application of riboflavin drops, (2) variable precorneal permanence of riboflavin, and (3) non-uniform distribution of riboflavin film over the stromal surface.

The use of the novel theranostic UV-A device provided valuable information on the dynamics behaviour of intrastromal riboflavin consumption during UV-A irradiation of human corneal tissues. Two different photochemical mechanisms, of which one is favoured at low oxygen

concentration (type I) and the latter is favoured in the presence of oxygen (type II), are currently known to be involved in the formation of additional cross-linking bonds between the stromal proteins during riboflavin/UV-A corneal cross-linking [36, 37]. In the type I mechanism, by receiving energy from UV-A light, riboflavin becomes the excited riboflavin triplet, which interacts directly with the substrate (ie, stromal proteins); in the type II mechanism, the excited riboflavin triplet reacts with oxygen dissolved in stroma to produce reactive oxygen species, including singlet oxygen, hydroxyl radical and hydrogen peroxide, which generate photo-oxidation and photo-polymerization of the substrate. The exponential decrease of intrastromal riboflavin concentration during UV-A illumination (see Figures 2 and 3) is consistent with the knowledge that the consumption of riboflavin in the stroma is spatially homogeneous and temporally monotonic decreasing [13, 14, 19, 32]. Since the intrastromal riboflavin concentration is

TABLE 2 Corneal intrastromal riboflavin concentration immediately after stromal soaking (C_{post}), after UV-A irradiation of the cornea ($C_{\text{UV-A}3\text{mW}}$) and their relative consumption are shown together with the values of Young's modulus of corneal tissue before (pre-operative) and after UV-A irradiation (post-operative). The relative increase of the Young's modulus with respect to the pre-operative values are also shown

Corneal tissue	Intrastromal riboflavin concentration			Young's modulus		Increase of Young's modulus (d.u.)
	C_{post} (10^{-4} g/cm ³)	$C_{\text{UV-A}3\text{mW}}$ (10^{-4} g/cm ³)	Consumption (%)	Preoperative (MPa)	Post-operative (MPa)	
142 875	1.80	0.60	65	1.16	1.63	1.40
143 104	1.80	0.60	66	2.86	3.82	1.34
143 455	1.60	0.47	70	1.25	1.99	1.58
143 712	1.70	0.22	86	2.23	2.83	1.27
151 714	1.60	0.21	86	1.13	1.61	1.42
151 715	1.70	0.18	89	1.40	2.2	1.56
157 111	1.70	0.98	42	1.50	1.53	1.02
157 122	1.60	0.80	50	1.60	1.78	1.11
157 133	1.40	0.89	46	1.55	1.62	1.05
157 144	1.40	0.33	76	1.45	1.80	1.24
M ± SD	1.6 ± 0.1	0.5 ± 0.3	68% ± 17%	1.61 ± 0.53	2.08 ± 0.72	1.30 ± 0.2

relatively low ($\leq 0.02\%$), the overall photochemical process can be considered as pseudo-first order under anaerobic conditions [22]; as a consequence, an exponential kinetic consumption of riboflavin is expected [22]. This implies that, in ambient environment (ie, 21% partial pressure of oxygen), the role of type I mechanism is predominant for the formation of additional chemical bonds between stromal proteins in riboflavin/UV-A corneal cross-linking with 30 minutes of stromal soaking with dextran-enriched riboflavin and total UV-A energy dose of 5.4 J/cm^2 using 3 mW/cm^2 power density. Previous authors have investigated whether the treatment would be oxygen-dependent or not providing controversial results [22, 37–39]. Sel et al. [38] have shown that riboflavin generates, via hydrogen peroxide formation during UV-A irradiation, hydroxyl radicals in ambient environment; the formation of these radicals has been shown to decrease with decreased riboflavin concentration. Richoz et al. [39] have shown that, in a controlled low oxygen environment (0.5% oxygen concentration in helium atmosphere), the biomechanical strengthening of the cornea induced by riboflavin/UV-A cross-linking is highly decreased in comparison with ambient environment (21% oxygen concentration). However, the authors neglected that corneal cross-linking is performed at oxygen environment of ambient air and the results of their work cannot be translated to the clinic. Kamaev et al. [22] have demonstrated that the main mechanism of the corneal cross-linking treatment is the direct interaction between riboflavin triplets and reactive groups of stromal proteins, which leads to the cross-linking of the proteins through radical reactions. However, the type II mechanism has been considered predominant at the start of UV-A illumination. McCall et al. [37] have assumed that riboflavin/UV-A corneal cross-linking is inhibited if singlet oxygen is quenched and stromal carbonyl groups are blocked, thus indicating the absence of other cross-linking mechanisms. On the other hand, these authors have used sodium azide to quench singlet oxygen, but this salt has been previously shown to quench riboflavin triplet as well [40, 41]. Huang et al. [42] have shown that singlet oxygen quencher alone cannot protect the riboflavin under light from degradation completely and have concluded that mixed type I and type II pathways are involved in the riboflavin degradation under light. Overall, the use of type I or type II pathways is dependent on the type and concentration of photosensitizer, concentrations of substrate, presence of enhancers and/or quenchers, and concentration and solubility of oxygen, which is higher in non-polar environments and lower in water-based systems. Since all the above experiments were carried out under different environment conditions and using different techniques or sample species, a direct comparison of results between studies remains challenging. From the present findings, at oxygen environment of ambient air, the main limiting factor for

effectively improving the biomechanical strength of the human corneal stroma during conventional corneal cross-linking is the intrastromal concentration of riboflavin prior to UV-A irradiation and its effective consumption during UV-A irradiation. Further studies are needed in order to understand the effect of epithelium or other UV-A irradiation protocols (ie, $\geq 9 \text{ mW/cm}^2$ with 5.4 J/cm^2 or higher energy density or intermittent UV-A light illumination) on the kinetics of corneal cross-linking with riboflavin [30].

Confocal imaging could theoretically improve the UV-A device's axial resolution and allow for analysis of intrastromal riboflavin at increasing depth of the cornea; on the other hand, the concentration of riboflavin has been shown to be almost constant up to 320 to 350 μm stromal depth [13, 32] (keratoconus corneas have in general stromal thickness thinner than 400 μm) and the effect of biomechanical strengthening has been measured to be mainly limited to the anterior 250 μm stromal depth [9–11, 35]. Therefore, increasing complexity in the system would not lead to a real advantage in the outcome measures.

5 | CONCLUSION

We have developed an image-guided innovative solution for estimating corneal cross-linking efficacy in real time through non-invasive measurement of intrastromal riboflavin concentration. Clinical studies are required in order to clarify whether this theranostic UV-A device may support corneal surgeons to successfully perform personalized corneal cross-linking treatments, ensuring safety and efficacy in every patient eye.

ACKNOWLEDGMENTS

We are thankful to Giovanni Desiderio (Consiglio Nazionale delle Ricerche, Istituto di Nanotecnologia, Rende, Italy), Roberto Caruso and Giuseppe Lupò (Consiglio Nazionale delle Ricerche, Istituto per i Processi Chimico Fisici, Messina, Italy) for their support in developing the theranostic device's electronic board and Domenico Arigò and Giuseppe Spinella (Consiglio Nazionale delle Ricerche, Istituto per i Processi Chimico Fisici, Messina, Italy) for their support in assembling the device and Chiara Mustarelli (Consiglio Nazionale delle Ricerche, Istituto Nazionale di Ottica) for assistance in preparing documents for ethical committee approval.

Conflict of interest

M.L. and G.L. are co-founders and shareholders of Vision Engineering Italy srl. G.L., N.L.M., V.V. and M.L. are co-inventors on a pending patent application (WO2017 130043A1) related to this work.

AUTHOR BIOGRAPHIES

Please see Supporting Information online.

ORCID

Giuseppe Lombardo  <http://orcid.org/0000-0002-9416-967X>

REFERENCES

- [1] A. Gordon-Shaag, M. Millodot, E. Shneur, Y. Liu, *Biomed. Res. Int.* **2015**, 2015, Article ID 795738, 19.
- [2] J. Wheeler, M. A. Hauser, N. A. Afshari, R. R. Allingham, Y. Liu, *Reprod. Syst. Sex. Disord.* **2012**, *S6*, 1.
- [3] C. N. J. McGhee, *Clin. Exp. Optom.* **2013**, *96*, 137.
- [4] I. M. Y. Cheung, N. J. N. McGhee, T. Sherwin, *Clin. Exp. Optom.* **2013**, *96*, 188.
- [5] E. Chan, G. R. Snibson, *Clin. Exp. Optom.* **2013**, *96*, 155.
- [6] K. M. Meek, S. Hayes, *Ophthalmic Physiol. Opt.* **2013**, *33*, 78.
- [7] J. B. Randleman, S. S. Khandelwal, F. Hafezi, *Surv. Ophthalmol.* **2015**, *60*, 509.
- [8] F. Raiskup-Wolf, A. Hoyer, E. Spoerl, L. E. Pillunat, *J. Cataract Refract. Surg.* **2008**, *34*, 796.
- [9] I. M. Beshtawi, C. O'Donnell, H. Radhakrishnan, *J. Cataract Refract. Surg.* **2013**, *39*, 451.
- [10] M. Kohlhaas, E. Spoerl, T. Schilde, G. Unger, C. Wittig, L. E. Pillunat, *J. Cataract Refract. Surg.* **2006**, *32*, 279.
- [11] C. Labate, M. P. De Santo, G. Lombardo, M. Lombardo, *PLoS One* **2015**, *10*, e0122868.
- [12] S. Kling, L. Remon, A. Pérez-Escudero, J. Merayo-Llodes, S. Marcos, *Invest. Ophthalmol. Vis. Sci.* **2010**, *51*, 3961.
- [13] M. Lombardo, N. Micali, V. Villari, S. Serrao, G. Lombardo, *Invest. Ophthalmol. Vis. Sci.* **2016**, *57*, 476.
- [14] M. Lombardo, N. Micali, V. Villari, S. Serrao, G. Pucci, R. Barberi, G. Lombardo, *J. Cataract Refract. Surg.* **2015**, *41*, 2283.
- [15] C. Wittig-Silva, E. Chan, F. M. A. Islam, T. Wu, M. Whiting, G. R. Snibson, *Ophthalmology* **2014**, *121*, 812.
- [16] Y. Goldich, A. L. Marcovich, Y. Barkana, Y. Mandel, A. Hirsh, Y. Morad, I. Avni, D. Zadok, *Cornea* **2012**, *31*, 609.
- [17] F. Raiskup, E. Spoerl, *Ocul. Surf.* **2013**, *11*, 93.
- [18] H. El Rami, E. Chelala, A. Dirani, A. Fadlallah, A. Fakhoury, C. Cherfan, G. Cherfan, E. Jarade, *Biomed. Res. Int.* **2015**, 2015, 7.
- [19] L. Mastropasqua, M. Nubile, E. Calienno, P. A. Mattei, E. Pedrotti, N. Salgari, R. Mastropasqua, M. Lanzini, *Am. J. Ophthalmol.* **2014**, *157*, 623.
- [20] A. P. Søndergaard, J. Hjortdal, T. Breitenbach, A. Ivarsen, *Curr. Eye Res.* **2010**, *35*, 116.
- [21] M. D. Friedman, R. Pertaub, D. Usher, E. Sherr, P. Kamaev, D. Muller, *J. Ophthalmol.* **2012**, 2012, 6.
- [22] P. Kamaev, M. D. Friedman, E. Sherr, D. Muller, *Invest. Ophthalmol. Vis. Sci.* **2012**, *53*, 2360.
- [23] G. El Masry, D.-W. Sun, Principles of hyperspectral imaging technology. in *Hyperspectral Imaging for Food Quality Analysis and Control* (Ed. Da-Wen Sun), Academic Press, San Diego **2010**, p. 3.
- [24] N. Angelini, N. Micali, V. Villari, P. Mineo, D. Vitalini, E. Scamporrino, *Phys. Rev. E* **2005**, *71*, 021915.
- [25] A. Mazzaglia, A. Valerio, V. Villari, A. Rencurosi, L. Lay, S. Spadaro, L. M. Scolaro, N. Micali, *New J. Chem.* **2006**, *30*, 1662.
- [26] M. Lombardo, G. Lombardo, G. Carbone, M. P. De Santo, R. Barberi, S. Serrao, *Invest. Ophthalmol. Vis. Sci.* **2012**, *53*, 1050.
- [27] C. Labate, M. Lombardo, M. P. De Santo, J. Dias, N. Ziebarth, G. Lombardo, *Invest. Ophthalmol. Vis. Sci.* **2015**, *56*, 4053.
- [28] H. J. Butt, B. Cappella, M. Kappl, *Surf. Sci. Rep.* **2005**, *59*, 1.
- [29] M. A. Poggi, *Anal. Chem.* **2005**, *77*, 1192.
- [30] M. Lombardo, G. Pucci, R. Barberi, G. Lombardo, *J. Cataract Refract. Surg.* **2015**, *41*, 446.
- [31] H. P. Iseli, M. Popp, T. Seiler, E. Spoerl, M. Mrochen, *J. Refract. Surg.* **2010**, *27*, 195.
- [32] E. Spoerl, F. Raiskup, D. Kampik, G. Geerling, *Curr. Eye Res.* **2010**, *35*, 1040.
- [33] S. Hayes, S. R. Morgan, D. P. O'Brart, N. O'Brart, K. M. Meek, *Acta Ophthalmol.* **2016**, *94*, e109.
- [34] T. A. Alhamad, D. P. O'Brart, N. A. O'Brart, K. M. Meek, *J. Cataract Refract. Surg.* **2012**, *38*, 884.
- [35] I. M. Beshtawi, R. Akhtar, M. C. Hillarby, C. O'Donnell, X. Zhao, A. Brahma, F. Carley, B. Derby, H. Radhakrishnan, *Invest. Ophthalmol. Vis. Sci.* **2014**, *55*, 1549.
- [36] K. Reiser, R. J. McCormick, R. B. Rucker, *FASEB J.* **1992**, *6*, 2439.
- [37] A. S. McCall, S. Kraft, H. F. Edelhauser, G. W. Kidder, R. R. Lundquist, H. E. Bradshaw, Z. Dedeic, M. J. Dionne, E. M. Clement, G. W. Conrad, *Invest. Ophthalmol. Vis. Sci.* **2010**, *51*, 129.
- [38] S. Sel, N. Nass, S. Pötzsch, S. Trau, A. Simm, T. Kalinski, G. I. W. Duncker, F. E. Kruse, G. U. Auffarth, H.-J. Brömme, *Redox Rep.* **2014**, *19*(2), 72.
- [39] O. Richo, A. Hammer, D. Tabibian, Z. Gatziofias, F. Hafezi, *Trans. Vis. Sci. Tech.* **2013**, *2*, 6.
- [40] C. Lu, W. Lin, W. Wang, Z. Han, S. Yao, N. Lin, *Phys. Chem. Chem. Phys.* **2000**, *2*, 329.
- [41] J. D. Spikes, H. R. Shen, P. Kopeckova, J. Kopecek, *Photochem. Photobiol.* **1999**, *70*, 130.
- [42] R. Huang, E. Choe, D. B. Min, *J. Food Sci.* **2004**, *69*, C726.

How to cite this article: Lombardo G, Villari V, Micali NL, et al. Non-invasive optical method for real-time assessment of intracorneal riboflavin concentration and efficacy of corneal cross-linking. *J. Biophotonics*. 2018;e201800028. <https://doi.org/10.1002/jbio.201800028>